blood®
Regular Article

MYELOID NEOPLASIA

Physiological *Srsf2* P95H expression causes impaired hematopoietic stem cell functions and aberrant RNA splicing in mice

Ayana Kon,[1] Satoshi Yamazaki,[2] Yasuhito Nannya,[1] Keisuke Kataoka,[1] Yasunori Ota,[3] Masahiro Marshall Nakagawa,[1] Kenichi Yoshida,[1] Yusuke Shiozawa,[1] Maiko Morita,[2] Tetsuichi Yoshizato,[1] Masashi Sanada,[4] Manabu Nakayama,[5] Haruhiko Koseki,[6] Hiromitsu Nakauchi,[2,7,*] and Seishi Ogawa[1,*]

[1]Department of Pathology and Tumor Biology, Graduate School of Medicine, Kyoto University, Kyoto, Japan; [2]Division of Stem Cell Therapy, Center for Stem Cell Biology and Medicine and [3]Department of Pathology, Research Hospital, Institute of Medical Science, University of Tokyo, Tokyo, Japan; [4]Clinical Research Center, National Hospital Organization, Nagoya Medical Center, Nagoya, Japan; [5]Chromosome Engineering Team, Department of Technology Development, Kazusa DNA Research Institute, Kisarazu, Japan; [6]Laboratory for Developmental Genetics, RIKEN Center for Integrative Medical Sciences, Yokohama, Japan; and [7]Institute for Stem Cell Biology and Regenerative Medicine, Stanford University School of Medicine, Stanford, CA

KEY POINTS

- **Blood-specific expression of the *Srsf2* P95H mutant results in decreased stem/progenitor cell numbers and a reduced repopulation capacity.**
- ***Srsf2* P95H mutation by itself is not sufficient to develop MDS but contributes to the MDS phenotype in transplantation settings.**

Splicing factor mutations are characteristic of myelodysplastic syndromes (MDS) and related myeloid neoplasms and implicated in their pathogenesis, but their roles in the development of MDS have not been fully elucidated. In the present study, we investigated the consequence of mutant *Srsf2* expression using newly generated *Vav1-Cre*–mediated conditional knockin mice. Mice carrying a heterozygous *Srsf2* P95H mutation showed significantly reduced numbers of hematopoietic stem and progenitor cells (HSPCs) and differentiation defects both in the steady-state condition and transplantation settings. *Srsf2*-mutated hematopoietic stem cells (HSCs) showed impaired long-term reconstitution compared with control mice in competitive repopulation assays. Although the *Srsf2* mutant mice did not develop MDS under the steady-state condition, when their stem cells were transplanted into lethally irradiated mice, the recipients developed anemia, leukopenia, and erythroid dysplasia, which suggests the role of replicative stress in the development of an MDS-like phenotype in *Srsf2*-mutated mice. RNA sequencing of the *Srsf2*-mutated HSPCs revealed a number of abnormal splicing events and differentially expressed genes, including several potential targets implicated in the pathogenesis of hematopoietic malignancies, such as *Csf3r*, *Fyn*, *Gnas*, *Nsd1*, *Hnrnpa2b1*, and *Trp53bp1*. Among the mutant *Srsf2*-associated splicing events, most commonly observed were the enhanced inclusion and/or exclusion of cassette exons, which were caused by the altered consensus motifs for the recognition of exonic splicing enhancers. Our findings suggest that the mutant *Srsf2* leads to a compromised HSC function by causing abnormal RNA splicing and expression, contributing to the deregulated hematopoiesis that recapitulates the MDS phenotypes, possibly as a result of additional genetic and/or environmental insults. (*Blood*. 2018;131(6):621-635)

Introduction

Myelodysplastic syndromes (MDS) and related neoplasms, including chronic myelomonocytic leukemia (CMML), are stem cell–derived chronic myeloid neoplasms, characterized by abnormal blood cell morphologic status and ineffective hematopoiesis leading to blood cytopenias (myelodysplasia).[1] Progression to secondary acute myeloid leukemia is common and is found in approximately one-third of patients.[2] As for their pathogenesis, high-throughput genomic studies of recent years have revealed frequent pathway mutations involving multiple components of the RNA splicing machinery in myelodysplasia, which have been shown to be among the most frequently mutated classes of genes in these neoplasms.[3,4] Largely occurring in a mutually exclusive manner, most of these mutations affect the components that are involved in the initial steps of premessenger RNA splicing, including *SF3B1*, *SRSF2*, *U2AF1*, and *ZRSR2*, which suggest their common effect on RNA splicing in the pathogenesis of myelodysplasia.[5]

Among frequently mutated splicing factors (SFs), SRSF2 is a member of the serine/arginine (SR) family of proteins that is characterized by 1 or 2 RNA recognition motifs (RRMs) and a serine/arginine-rich (RS) domain. SRSF2 binds RNA motifs known as exonic splicing enhancers within the target exon through an

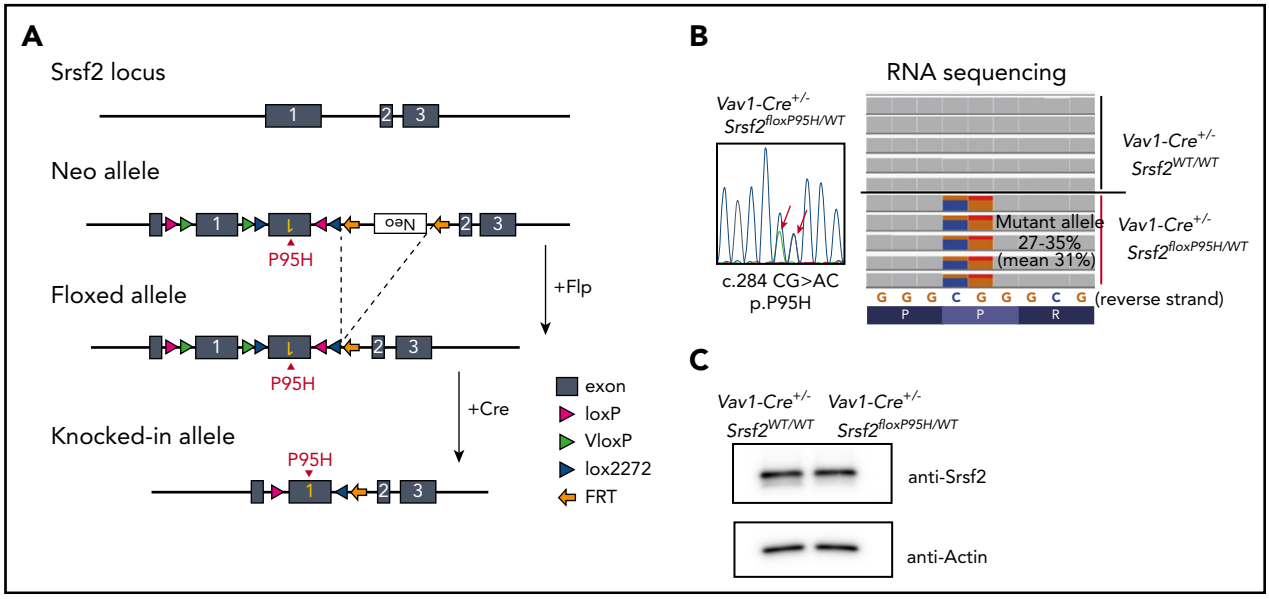

Figure 1. Generation of *Srsf2* P95H conditional knockin mice. (A) Schematic representation of the targeted *Srsf2* allele. (B) Sanger sequencing of polymerase chain reaction products of cDNA of the BM cells from *Vav1-Cre*$^{+/-}$*Srsf2*$^{floxP95H/WT}$ mice (left), and RNA-seq of KSL cells of *Vav1-Cre*$^{+/-}$*Srsf2*$^{WT/WT}$ and *Vav1-Cre*$^{+/-}$*Srsf2*$^{floxP95H/WT}$ mice (right). (C) Western blot analysis of the expression of Srsf2 in the BM-derived nucleated cells of *Vav1-Cre*$^{+/-}$*Srsf2*$^{WT/WT}$ and *Vav1-Cre*$^{+/-}$*Srsf2*$^{floxP95H/WT}$ mice. FRT, flippase recognition target.

RRM and promotes inclusion or exclusion of that exon, playing an indispensable role in both constitutive and alternative splicing (AS) in most cell types.[6-8] Somatic mutations in *SRSF2* occur most frequently in CMML (28%-47%),[3-5,9,10] where *SRSF2* mutations represent one of the initiating events during MDS pathogenesis.[3,4,11] All *SRSF2* mutations are heterozygous and almost always affect the proline 95 residue within an intervening sequence between the RRMs and the RS domain, which suggests a neomorphic function of these mutations.

Recently, several studies have attempted to clarify the role of SF mutations in vivo. *Mx1-Cre*–mediated conditional knockin of the *Srsf2* P95H mutation impaired hematopoietic differentiation, increased hematopoietic stem and progenitor cells (HSPCs), and promoted myelodysplasia by altering the RNA-binding specificity of Srsf2 in mice.[12] The altered RNA-binding affinity of mutant SRSF2 and splicing changes were also demonstrated using leukemic cell lines expressing an *SRSF2* mutant allele.[13] Other groups have reported that mice models of the pathogenic mutations in *U2af1*[14] and *Sf3b1*[15,16] displayed defects in differentiation accompanied by RNA-splicing changes. These studies represent major advances toward understanding how SF mutations affect hematopoietic functions in myelodysplasia. However, given that the hematological phenotypes were investigated only in transplantation settings in the published *Srsf2* knockin mice model,[12] it is unclear to what extent the observed phenotypes were ascribed to the effect of transplantation, which are known to cause considerable stress on hematopoietic cells and an altered bone marrow (BM) microenvironment. Thus, in this study, we investigated the hematological consequences of *Srsf2* mutation both under the steady-state condition and in a regenerative context using a newly generated *Vav1-Cre*–mediated conditional knockin mouse model of the *Srsf2* P95H mutation.

Materials and methods

Mice

We constructed the *Srsf2*-targeting vector using the "flip-excision" (FLEx) switch strategy as previously described.[17,18] The linearized vector was electroporated into murine hybrid (C57BL/6×129/Sv) embryonic stem cells. Chimeric mice were produced by microinjection of targeted embryonic stem cells into blastocysts and were bred to C57BL/6 mice to establish germ line transmission. Mice were backcrossed against C57BL/6 mice for at least 6 generations. All animal experiments were approved by the Animal Care and Use Committee of the Institute of Medical Science, the University of Tokyo, and Kyoto University. Full details are provided in supplemental Methods.

Flow cytometry and BM transplantation

Single-cell suspensions prepared from the BM, spleen, and peripheral blood (PB) were stained with monoclonal antibodies (supplemental Table 1). Purification of HSPCs was performed as previously described.[19] In competitive or noncompetitive BM transplantation, 1×10^6 freshly isolated BM cells were transplanted into lethally irradiated recipient mice with or without the same number of competitor BM cells. Full details are described in supplemental Methods.

RNA sequencing

We extracted total RNA using NucleoSpin RNA XS (Macherey-Nagel) from sorted cell populations from 17- to 21-week-old littermate *Srsf2* mutant and wild-type mice (steady-state) or recipient mice 3 to 6 months after noncompetitive BM transplantation. RNA samples with RNA integrity number >8 proceeded to the sequencing analysis. The synthesis and amplification of complementary DNA (cDNA) were performed using SMARTer Ultra Low Input RNA Kit for Sequencing, version 3 or 4 (Clontech). Sequencing libraries were generated using the Low Input Library Prep Kit

(Clontech), followed by high-throughput sequencing on the HiSeq 2500 System (Illumina) with 124 bp paired-end reads.

For the data analysis, the sequencing reads were aligned to the mouse reference genome (mm10) using HISAT2 (version 2.0.4).[20] To identify differential AS events, we applied rMATS[21] with the following parameters: anchor length 2, unpaired analysis type, and "unstranded" library type. Gene and transcript annotations were referred from "archive-2015-07-17-14-33-2" in the University of California Santa Cruz annotation archives. Splicing site sequences and their logos were analyzed with Bioconductor seqLogo library (version 3.3). For differential expression analysis, transcript read counts mapped to each gene were extracted using Rsubread package[22] and were compared using edgeR package.[23,24] RNA sequencing (RNA-seq) data have been deposited in the DNA Data Bank of Japan repository under accession number DRA006224.

Statistical analysis

We calculated *P* values comparing 2 means using the 2-tailed unpaired Student *t* test using GraphPad Prism, version 6. The log-rank test was used to compare the overall survival. We used the Fisher's exact test to determine the *P* values comparing the composition of SSNG motifs in the cassette exons (CEs). Statistical significance of the overlap between differentially spliced or expressed genes from different cell populations was estimated using Monte Carlo simulations.

Results

Reduced number of HSPCs with impaired differentiation in *Srsf2* mutant mice

To elucidate the role of *SRSF2* mutation in the development of myelodysplasia, we generated an *Srsf2P95H* conditional knock-in mouse using a FLEx switch strategy (Figure 1A).[18] We chose *Vav1-Cre* transgenic mice, instead of *Mx1-Cre* mice, as a Cre deleter strain to induce constitutive and hematopoietic-specific Cre expression[25] to exclude the proproliferative effects of interferon.[26,27] Mice heterozygous for the floxed *Srsf2P95H* allele were crossed with *Vav1-Cre* mice to obtain a cohort of *Vav1-Cre*$^{+/-}$*Srsf2*$^{floxP95H/WT}$ and control *Vav1-Cre*$^{+/-}$*Srsf2*$^{WT/WT}$ mice. *Vav1-Cre*$^{+/-}$*Srsf2*$^{floxP95H/WT}$ mice expressed nearly equal levels of *Srsf2P95H* (c.284CG>AC) and wild-type *Srsf2* alleles in hematopoietic cells, resulting in equivalent levels of Srsf2 protein expression compared with *Vav1-Cre*$^{+/-}$*Srsf2*$^{WT/WT}$ mice (Figure 1B-C). Successful recombination and expression of the *Srsf2P95H* allele were also confirmed by genotyping of multiple colonies (14/14) derived from single CD34$^-$KSL HSCs. Notably, *Vav1-Cre*–positive mice having homozygous *Srsf2*^{floxP95H} alleles were not obtained (0/43), which suggests the lethality of homozygous expression of the mutant *Srsf2* allele. Unexpectedly, however, we also failed to obtain the mice having homozygous floxed *Srsf2P95H* alleles, even under the *Vav1-Cre*–negative background (0/46), which suggests that the floxed *Srsf2P95H* allele was null or severely hypomorphic due to the FLEx switch design. In fact, *Vav1-Cre*–negative *Srsf2*$^{floxP95H/WT}$ mice were born normally, but RNA-seq of their BM cells revealed a low level of *Srsf2* expression from the floxed allele (~2.0% of that from the wild-type allele) (supplemental Figure 1A), although the mice had an apparently normal level of wild-type *Srsf2* expression with a trace amount of the mutant *Srsf2* reads (~1.1%), probably caused by spontaneous recombination. Thus, it was difficult to determine whether the lethality of *Vav1-Cre*–positive *Srsf2*$^{floxP95H/floxP95H}$ mice was due to homozygous expression of the mutant *Srsf2* allele in hematopoietic tissues or to the *Srsf2* deficiency in other tissues with low *Vav1* promoter activities, or to both.

None of the *Vav1-Cre*$^{+/-}$*Srsf2*$^{floxP95H/WT}$ mice developed MDS or other hematological malignancies at least by 90 weeks of age (0/20). There was no significant difference in overall survival between mutant and control mice (supplemental Figure 1B). *Vav1-Cre*$^{+/-}$*Srsf2*$^{floxP95H/WT}$ mice exhibited decreased hemoglobin levels with elevated levels of mean corpuscular volume (MCV) and mean corpuscular hemoglobin (MCH) compared with *Vav1-Cre*$^{+/-}$*Srsf2*$^{WT/WT}$ mice but otherwise showed grossly normal steady-state hematopoiesis (Figure 2A; supplemental Figure 1C). BM and spleen cellularity were similar between both mice, without showing morphologic abnormalities (Figure 2B; supplemental Figure 1D-F).

However, the absolute number of multipotent self-renewing HSCs characterized by low CD34 expression (CD34$^-$KSL cells) or c-Kit$^+$Sca-1$^+$Lin^{low}CD150$^+$CD48$^-$phenotype (long-term HSCs [LT-HSCs]) was significantly reduced in mutant mice compared with that of the control mice; the same trend was observed for immature hematopoietic progenitors, including KSL cells, CD34$^+$c-Kit$^+$Sca-1$^+$Lin^{low} (CD34$^+$KSL) cells, c-Kit$^+$Sca-1$^+$Lin^{low}CD150$^-$CD48$^-$cells (multipotent progenitors [MPPs]), and restricted hematopoietic progenitor cells (HPC-1; c-Kit$^+$Sca-1$^+$Lin^{low}CD150$^-$CD48$^+$) (Figure 2C-F).[28-30] The reduced number of HSCs in mutant mice was also demonstrated by limiting-dilution assays, in which the estimated number of multilineage repopulating cells of *Srsf2* wild-type and mutant mice was 1 in 4.0×10^4 and 2.3×10^5 BM cells, respectively (Figure 2G). Whereas the frequency of apoptotic cells among LT-HSCs and KSL cells was not significantly changed (supplemental Figure 1G), the proportion of quiescent HSPCs was significantly decreased in *Srsf2* mutant mice compared with control mice (Figure 2H), which indicates that the reduction in HSC numbers in mutant mice was due to the increase of the cycling HSCs. In contrast, there was no significant difference between mutant and control mice in the number of more differentiated progenitors, including common myeloid progenitors (CMPs; c-Kit$^+$Sca-1$^-$Lin^{low}CD34$^+$FcγR^{med}), granulocyte/macrophage lineage-restricted progenitors (GMPs; c-Kit$^+$Sca-1$^-$Lin^{low}CD34$^+$FcγR^{high}), megakaryocyte/erythrocyte lineage-restricted progenitors (MEPs; c-Kit$^+$Sca-1$^-$Lin^{low}CD34$^-$FcγR^{low}),[31] common lymphoid progenitors (CLPs; Lin^{low}IL-7Rα$^+$Flt3$^+$Sca-1^{med}c-Kit^{med}),[32,33] and erythroid progenitors (supplemental Figure 1H-J). Lineage distribution in the BM and the spleen cells did not differ substantially between mutant and control animals either, except for impaired differentiation of B-cell precursors in mutant mice (supplemental Figure 1K-L).

Reduced number of HSPCs and dysplastic hematopoiesis in *Srsf2* mutant transplanted mice

We next assessed the phenotype of *Srsf2*-mutated stem cells in transplantation settings to evaluate the effect of increasing replicative stress, which has been shown to substantially affect the behavior of normal and abnormal stem cells.[34-36] Mutant-derived BM cells reconstituted the recipient's hematopoiesis, in which more than 90% of PB cells were derived from donor

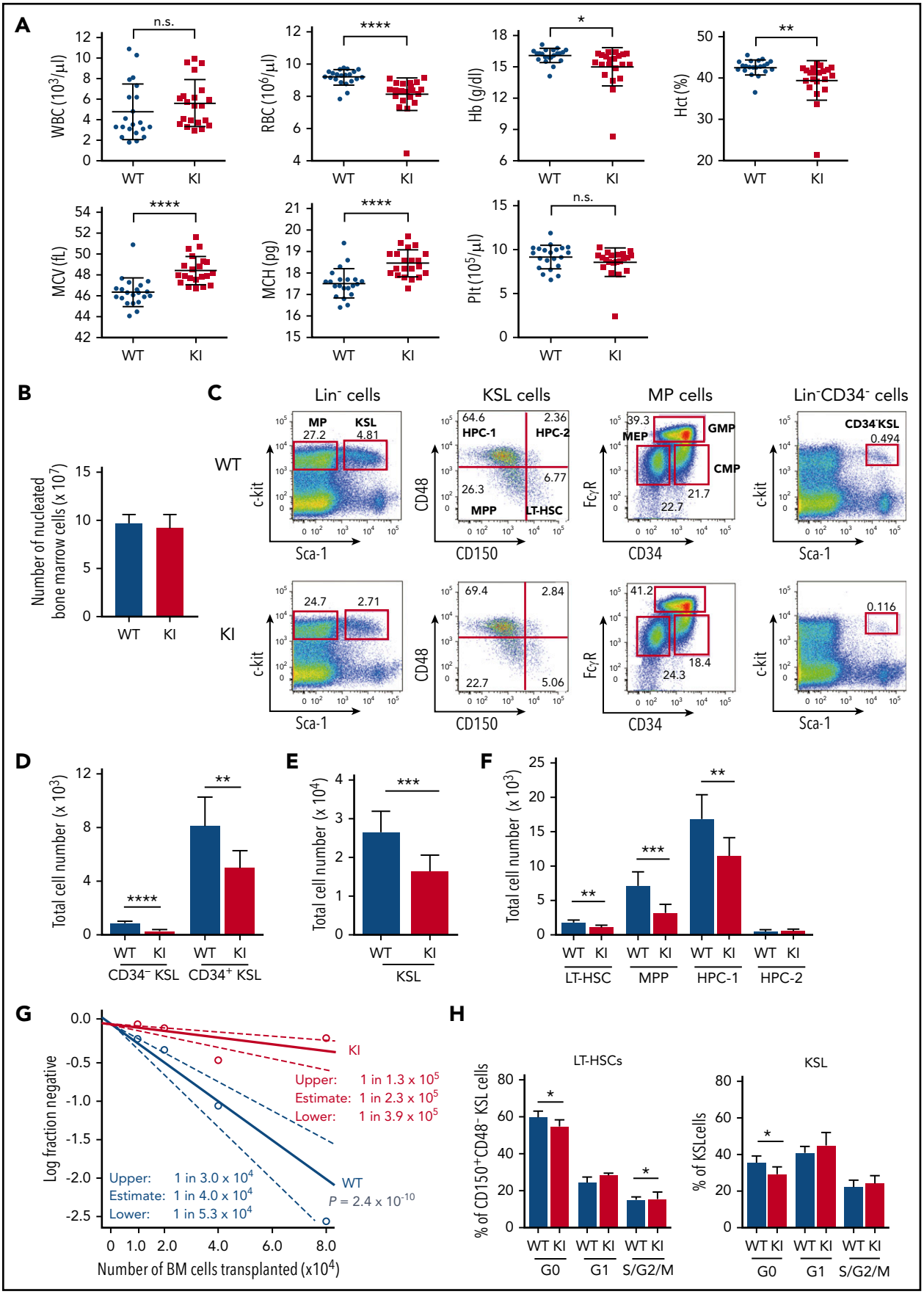

Figure 2.

cells at least until 16 weeks after transplantation (Figure 3A). In vivo homing assay using carboxyfluorescein succinimidyl ester (CFSE)–labeled BM-derived mononuclear cells showed no significant differences in the proportion of CFSE-positive cells in the recipient BM at 16 hours after transplantation, which suggests that mutant-derived BM cells largely retained normal homing capability (Figure 3B). There was no significant difference in BM cellularity between mutant and control transplanted mice, both displaying normocellular BM (Figure 3C). However, in agreement with the findings in the nontransplanted mice, flow cytometry of the BM from the mutant transplanted mice revealed a significant decrease in the numbers of stem and progenitor cells compared with the control transplanted mice. The reduced cell number was also observed in more mature hematopoietic fractions, including CMPs and CLPs (Figure 3D-H). The frequency of the cycling *Srsf2* mutant HSCs was substantially higher than those of wild-type HSCs, and the difference became more prominent in transplantation settings compared with those in the steady-state condition (Figure 2H; Figure 3I). In addition, *Srsf2* mutant HSCs showed a higher frequency of apoptosis, compared with wild-type HSCs (Figure 3J). The mutant transplanted mice showed an increase in the myeloid bias and impaired differentiation of B-cell precursors, as seen in human MDS (Figure 3K-L).[37]

The mutant transplanted mice also showed additional evidence of abnormal dysplastic hematopoiesis. Compared with the control transplanted mice, the mutant transplanted mice had lower white blood cell counts and macrocytic anemia and showed a significantly shorter survival time with no evidence of leukemic transformation, which suggests BM failure as the major cause of deaths (Figure 4A-B; supplemental Figure 2A). The mutant transplanted animals also exhibited a slight but significant increase in the number of dysplastic erythroid cells in the BM, including those with multiple nuclei, compared with the wild-type transplanted mice (Figure 4C-D). Flow cytometry of the spleen and BM cells based on CD71 and Ter119 expression[38] showed impaired erythroid differentiation (Figure 4E). The mutant transplanted mice demonstrated increased megakaryocytes in the spleen and increased paratrabecular megakaryocytes in the BM, which are characteristic of human MDS,[39] indicating the presence of dysplastic megakaryopoiesis (supplemental Figure 2B-C).

Compromised reconstitution capacity of *Srsf2*-mutated stem cells

To further characterize *Srsf2*-mutated stem cells, we evaluated the reconstitution capacity of these HSCs using competitive repopulation assays. Compared with the wild-type transplanted mice, the mutant transplanted mice showed a significant and progressive reduction in the chimerism of donor-derived cells in PB, which was seen in all lineages examined (Figure 5A-B). At 4 months after transplantation, the chimerism of mutant-derived cells in the BM HSPC fractions declined to very low levels compared with that of wild-type–derived cells (Figure 5C). We next performed serial transplantation assays to evaluate the repopulating capacity of highly primitive *Srsf2*-mutated HSCs, in which the chimerism of mutant-derived cells in PB further declined (Figure 5D). The reduced repopulating capacity of mutant-derived stem cells was also demonstrated with use of a highly purified fraction of $CD34^-$KSL HSCs (Figure 5E). To exclude a possibility of defective BM homing of mutant stem cells as the cause of reduced chimerism, we also performed an intra-BM competitive repopulation assay. We still observed the reduced chimerism of mutant-derived cells as early as 1 week after transplantation (Figure 5F), which supports the interpretation that the reduced chimerism of *Srsf2*-mutated HSCs was due to their impaired repopulating capacity.

Effect of the *Srsf2* P95H mutation on RNA splicing in vivo

We next evaluated the effect of mutant *Srsf2* on RNA splicing through transcriptome sequencing of KSL cells and MPs (c-Kit^+ Sca-1^-Lin^{low}) purified from the BM of *Vav1-Cre*$^{+/-}$ *Srsf2*$^{floxP95H/WT}$ and *Vav1-Cre*$^{+/-}$ *Srsf2*$^{WT/WT}$ mice, as well as mutant and wild-type transplanted mice. By using the rMATS algorithm[21] with a cutoff value of a false discovery rate (FDR) <0.1% and >5% for inclusion level differences, we identified 1484 and 1087 abnormal AS events in KSL and MP cells in transplantation settings, respectively, and 927 and 276 abnormal AS events in KSL and MP cells in the steady state, respectively. The types of abnormal AS events were consistent among all of the populations, in which the CEs were most frequently affected, followed by mutually exclusive exons, alternative 3′/5′ splice sites, and intron retentions. *Srsf2* mutations were associated with a mild bias toward exclusion of CEs, alternative splice sites, and intron retentions (Figure 6A-B; supplemental Figure 3A; supplemental Table 2). The magnitude of mutant-associated splicing changes remained at less than 20% of authentic splicing reads for most of the differentially spliced events (>70%) (supplemental Figure 3B). The validity of the detection was confirmed by quantitative reverse transcription polymerase chain reaction for several splicing junctions (supplemental Figure 4).

SRSF2 is known to promote inclusion or exclusion of exons through binding to specific exonic splicing enhancers,[6,40,41] in which 5′-SSNG-3′ (S=C/G, N=A/U/C/G) consensus motifs provide high-affinity binding sites.[8] Based on this knowledge, we investigated 4-mers that were significantly enriched in the CEs differentially spliced in *Srsf2*-mutated cells. Consistent with previous reports,[12,13] CCNG and GGNG were significantly enriched in those exons that were more included (splicing promoted) and excluded (splicing repressed) in the *Srsf2*-mutated

Figure 2. Reduced number of HSPCs with impaired differentiation in *Srsf2* mutant mice. (A) White blood cells (WBCs), red blood cells (RBCs), hemoglobin (Hb), hematocrit (Hct), MCV, MCH, and platelet (Plt) counts in PB from 8- to 15-week-old *Vav1-Cre*$^{+/-}$ *Srsf2*$^{WT/WT}$ (WT) and *Vav1-Cre*$^{+/-}$ *Srsf2*$^{floxP95H/WT}$ (KI) littermate male mice are plotted as dots (n = 21 per group). The mean ± standard deviation (SD) are indicated as bars. (B) Absolute numbers of nucleated BM cells in bilateral femurs and tibias from 12- to 15-week-old WT and KI male mice are shown as mean ± SD (n = 8). (C) Representative flow cytometry analysis of the BM stem and progenitor populations of WT and KI mice. (D-F) Total cell number of $CD34^-$KSLs and $CD34^+$KSLs (panel D); KSL cells (panel E); and LT-HSCs, MPPs, HPC-1, and HPC-2 (panel F) in the BM of 12- to 15-week-old mice (mean ± SD, n = 8). (G) Limiting-dilution analysis based on competitive repopulation 3 months after transplantation determined the frequency of multilineage repopulating cells in the BM. Data are expressed as mean and 95% confidence intervals for WT (n = 96 samples) and KI (n = 95 samples) combined from 4 independent experiments. Frequency and probability estimates were computed using the extreme limiting dilution analysis (ELDA) software (Bioinformatics). (H) Cell cycle analysis in LT-HSCs (c-Kit^+Sca-$1^+Lin^{low}CD150^+CD48^-$) and KSL cells using Ki-67 and Hoechst 33342 staining (mean ± SD, n = 6). *$P < .05$; **$P < .01$; ***$P < .001$; ****$P < .0001$. n.s., not significant.

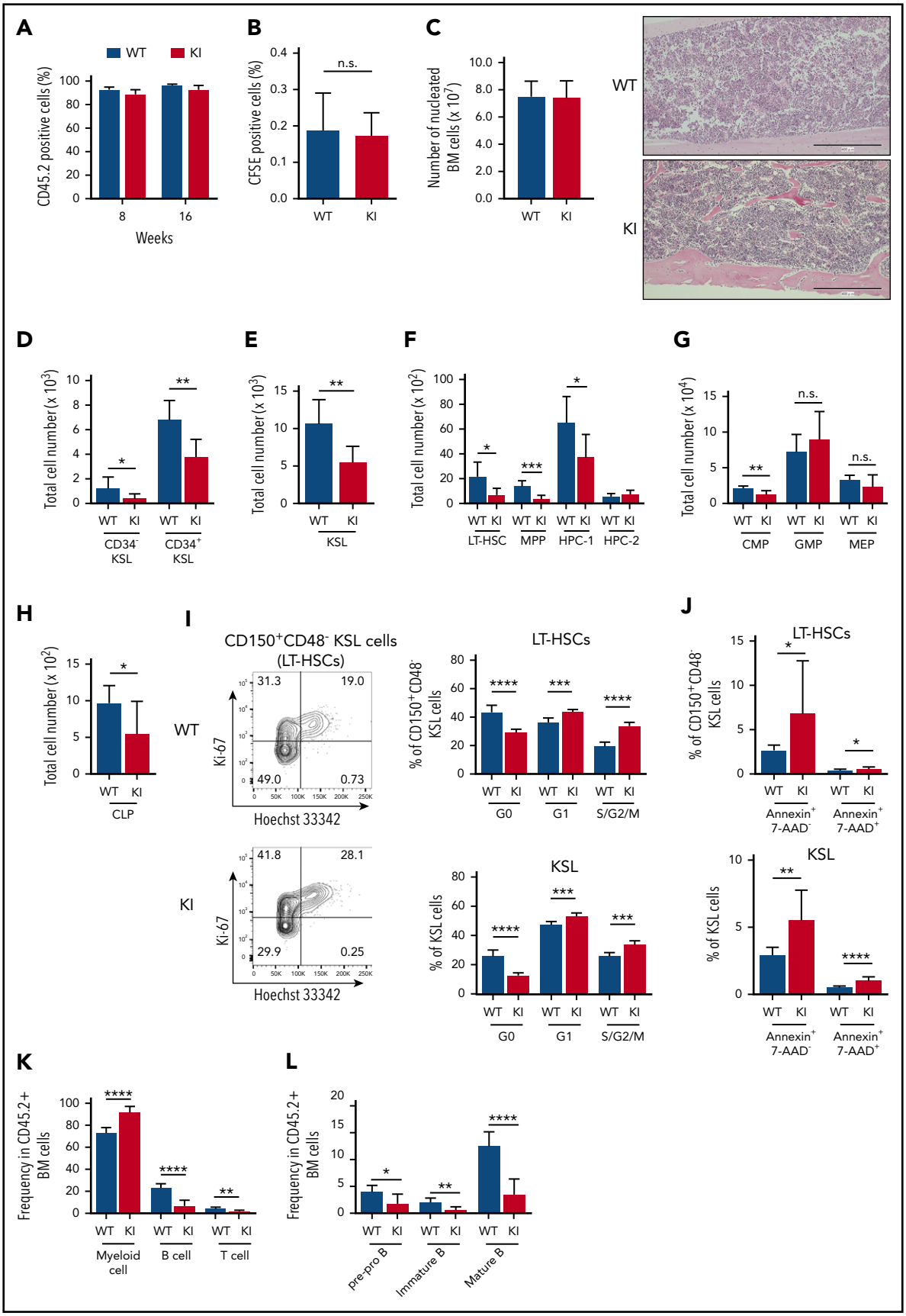

Figure 3. Consequences of *Srsf2* P95H mutation on hematopoiesis in transplantation settings. (A) The percentage of CD45.2$^+$ donor cells in the PB of WT and KI mice. Data are shown as mean ± SD from 3 independent experiments. The numbers of mice analyzed are n = 27 at 8 weeks and n = 21 at 16 weeks after transplantation. (B) The percentage of CFSE-positive cells in the BM of WT and KI mice at 16 hours after transplantation (mean ± SD, n = 5). (C) Left panel: absolute number of nucleated BM cells in bilateral femurs

cells, respectively, whereas no significantly different features in the intron-exon boundary sequences were identified between *Srsf2P95H*-promoted and *Srsf2P95H*-repressed exons (Figure 6C; supplemental Figure 3C-D). CCNG motifs tended to be slightly enriched in ~20 bp from the 3′ splice site of promoted exons compared with more distal upstream intronic regions, whereas GGNG motifs were enriched over the repressed CEs compared with their surrounding intronic regions (Figure 6D; supplemental Figure 3E).

Functional targets of the *Srsf2* P95H mutation

To identify the potential functional targets of mutant *Srsf2*, we interrogated differentially spliced genes between mutant and wild-type *Srsf2* for KSL and MP fractions in both the steady-state and transplantation settings. We identified a total of 1189 differentially spliced genes in at least one of the 4 fractions (Figure 6E). Among these, 98 genes were differentially spliced in more than 3 populations, of which 13 were registered in the Cancer Gene Census (http://cancer.sanger.ac.uk/census), such as *Hnrnpa2b1*, *Gnas*, *Atrx*, *Csf3r*, and *Mllt10* (Table 1). Higher numbers of abnormal AS events were observed in KSL and MP cells from *Srsf2* mutant transplanted mice, compared with those from steady-state mice. These AS events affected several genes implicated in leukemogenesis (*Stag2*, *Bap1*, and *Ctcf*), DNA damage response (*Chek2*, *Fancc*, *Rad51b*, and *Cdk4*), and apoptosis (*Casp8*) (Figure 6E). We also explored those genes showing significant changes in gene expression levels between *Srsf2* mutant and wild-type and identified 387 upregulated and 548 downregulated genes, with FDR <0.05 and >1.2-fold change, in at least one of the 4 populations, including *Hnrnpa2b1* and *Gata1* (upregulated) and *Mpl*, *Irf4*, *Csf3r*, and *Trp53bp1* (downregulated) (Figure 6F-G; supplemental Figure 3F; supplemental Table 3). Gene set enrichment analysis[42,43] revealed significant enrichment of pathways deregulated in human MDS[44] in *Srsf2* mutant KSL cells of transplanted recipients but not in those of nontransplanted mice. *Srsf2* mutant HSPCs also showed significant enrichment of several pathways, including loss of stemness, enhanced cell cycle and DNA repair, impaired differentiation, and upregulation of the genes involved in RNA metabolism both in the steady-state and transplantation settings (Figure 6H; supplemental Table 4). We detected no statistically significant overlaps between the differentially expressed genes and differentially spliced genes in any of the 4 cell fractions. Although only a small number of misspliced genes were predicted to be degraded by the nonsense-mediated decay pathway among the downregulated genes (supplemental Figure 5), several genes showed significant changes in both RNA splicing and expression, including *Hnrnpa2b1*, *Csf3r*, and *Trp53bp1*.

We next compared our results with those obtained from previous studies in a different mouse model and a human cell line.[12,13] To minimize potential biases from the analysis platform, we reanalyzed original RNA-seq data from a *Mx1-Cre Srsf2*^{P95H} mouse model[12] and *SRSF2* mutant K562 cells[13] using the same algorithm (rMATS) and cutoff points that we adopted for the analysis of our mouse model (supplemental Table 5). There were significant overlaps between the targets detected in our study compared with those of previous studies, which support the validity of the our current result. Among the 895 genes undergoing abnormal AS in KSL and/or MP cells in transplantation settings in our mouse model, 147 and 126 were also identified in the analysis of KSL cells ($P < 10^{-6}$) and MP cells ($P < 10^{-6}$) from different *Srsf2*-mutated mouse strains,[12] respectively (Figure 7A). Also, among the misspliced genes in KSL and/or MP cells in transplantation settings, 105 and 104 genes were overlapped with the targets identified in *SRSF2*-mutated primary human leukemia samples ($P < 10^{-6}$)[12] and a cell line transduced with mutant *SRSF2* ($P < 10^{-6}$),[13] respectively (Figure 7B). In addition to the previously reported targets, we newly identified a number of novel target genes of abnormal AS events, such as *Stag2* and *Setd2*. Genes that were differentially spliced in both mutant mouse strains and human samples included several genes implicated in the pathogenesis of myeloid malignancies; these include *Csf3r, Fyn, Gnas, and Nsd1*.[45-49] Among the CEs altered in both KSL and MP cells but not in human samples, approximately half had corresponding transcripts in the human orthologs; for those CEs, the frequency of CCNG motifs within the promoted CEs and GGNG motifs within the repressed CEs was decreased in human counterparts, which may in part account for the different splicing patterns between species (Figure 7C).

Previously, Kim et al[12] reported that *SRSF2* mutant cells exhibited preferential inclusion of a poison CE that introduces a premature termination codon predicted to trigger nonsense-mediated decay of *EZH2*. However, in the present study, we did not detect those CEs whose splicing pattern was significantly different between wild-type and mutant cells, not only in HSPCs but in more differentiated fractions, including what corresponds to the exon reported to be increased in human *EZH2* and in those reported to be changed in mice (supplemental Figure 6A-B). No significant difference was detected in the Ezh2 protein levels either (supplemental Figure 6C). We found two CCNG motifs within the *EZH2* poison CEs in human samples, in contrast to one CCNG motif in the mouse counterpart (supplemental Figure 6D), which may account for the discrepancy between the species.

Discussion

Effects of SF mutations on hematopoiesis were first examined by Yoshida et al,[5] using competitive transplantation of purified mouse stem cells transduced with different *U2AF1* mutants (S34F, Q157P, and Q157R). More recently, other groups have investigated *Mx1-Cre*–mediated conditional knockin mouse models of the *Srsf2*(P95H)[12] and the *Sf3b1*(K700E)[15,16] mutants,

Figure 3 (continued) and tibias from WT and KI mice. Right panel: Section of femurs stained with hematoxylin and eosin. Scale bars, 400 μm. (D-H) Total cell number of donor-derived CD45.2$^+$ CD34$^-$KSLs and CD34$^+$KSLs (panel D); KSL cells (panel E); LT-HSCs, MPPs, HPC-1, and HPC-2 (panel F); myeloid progenitors (panel G); and CLPs (panel H) in the BM (mean ± SD, n = 7). (I) Cell cycle analysis in donor-derived LT-HSCs and KSL cells using Ki-67 and Hoechst 33342 staining (mean ± SD, n = 6). (J) Percentage of apoptotic cells in donor-derived LT-HSCs and KSL cells (mean ± SD: WT, n = 10; KI, n = 9). (K) Percentages of myeloid (Gr-1$^+$ and/or Mac-1$^+$), B-lymphoid (B220$^+$), and T-lymphoid (CD4$^+$ and/or CD8$^+$) cells in the donor-derived CD45.2$^+$ nucleated BM cells (mean ± SD, n = 7). (L) Percentages of pre-pro B (CD19$^+$ B220$^+$ IgM$^-$), immature B (CD19$^+$ B220^{mid} IgM$^+$), and mature B (CD19$^+$ B220^{high} IgM$^+$) populations in the donor-derived CD45.2$^+$ nucleated BM cells (mean ± SD, n = 7). In panels C through L, mice were analyzed at 15 to 20 weeks after transplantation. *$P < .05$; **$P < .01$; ***$P < .001$; ****$P < .0001$. IgM, immunoglobulin M. KI, *Srsf2* mutant transplanted mice; WT, wild-type transplanted mice.

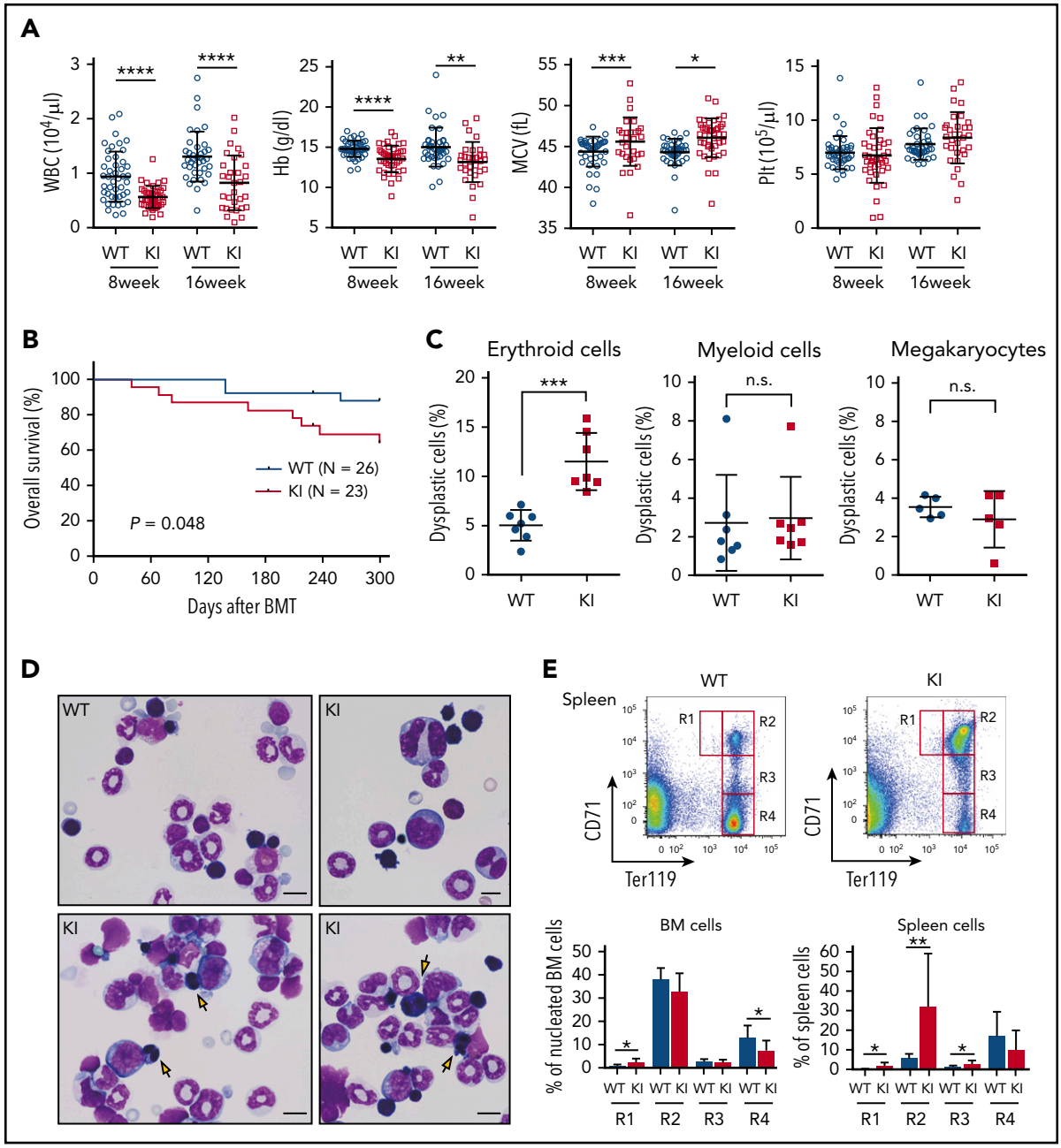

Figure 4. Abnormal dysplastic hematopoiesis in *Srsf2* mutant-transplanted mice. (A) Complete blood cell (CBC) counts of the PB from WT and KI mice are plotted as dots. The mean ± SD are presented as bars. Data were obtained from 4 independent experiments. The numbers of mice analyzed were n = 45 (WT) and n = 41 (KI) at 8 weeks and n = 38 (WT) and 31 (KI) at 16 weeks after transplantation. (B) Kaplan-Meier survival curve of WT (n = 26) and KI (n = 23) mice at 300 days after transplantation. (C) Percentages of dysplastic erythroid cells, myeloid cells, and megakaryocytes are plotted; bars indicate mean ± SD. In total, 7 pairs of WT and KI mice were analyzed for morphological evaluation of erythroid and myeloid cells, and 5 pairs were analyzed for morphological evaluation of megakaryocytes. For each mouse, >200 erythroid cells, >100 myeloid cells, and >15 megakaryocytes were counted. (D) Representative May–Grünwald–Giemsa staining of BM cells is shown; arrows point to binucleated erythroid cells. Magnification 1000×; scale bar, 10 μm. (E) Upper panels: representative flow cytometry analysis of erythroid lineage in the spleen, showing CD71^{high}Ter119^{med} (R1), CD71^{high}Ter119^{high} (R2), CD71^{med}Ter119^{high} (R3), and CD71^{low}Ter119^{high} (R4) gates. Lower panels: percentage of erythroid precursors in the BM and spleen cells (mean ± SD, n = 7). *P < .05; **P < .01; ***P < .001; ****P < .0001. BMT, bone marrow transplantation. KI, *Srsf2* mutant transplanted mice; WT, wild-type transplanted mice.

as well as a doxycycline-inducible transgenic mouse model for the *U2Af1*(S34F) mutant.[14] In all of these studies, SF-mutated HSCs exhibited a compromised repopulation capacity compared with wild-type HSCs, which were also recapitulated in our *Vav1-Cre*–inducible *Srsf2* mutant mice. Thus, one of the common consequences of *Srsf2* and other SF mutations seem to be compromised HSC function in terms of repopulating capacity. Given that SF mutations are implicated in early genetic events in myeloid leukemogenesis[3,4,11] and in clonal hematopoiesis in aged-normal populations (age-related clonal hematopoiesis [ARCH] or clonal hematopoiesis with indeterminate potential [CHIP]),[50-54] this trend raises a perplexing question: How can these functionally compromised HSCs harboring SF mutations be clonally selected in the early stages in leukemogenesis and ARCH/CHIP? Differential effects of these mutations on aged and nonaged stem cells and/or an abnormal BM environment that

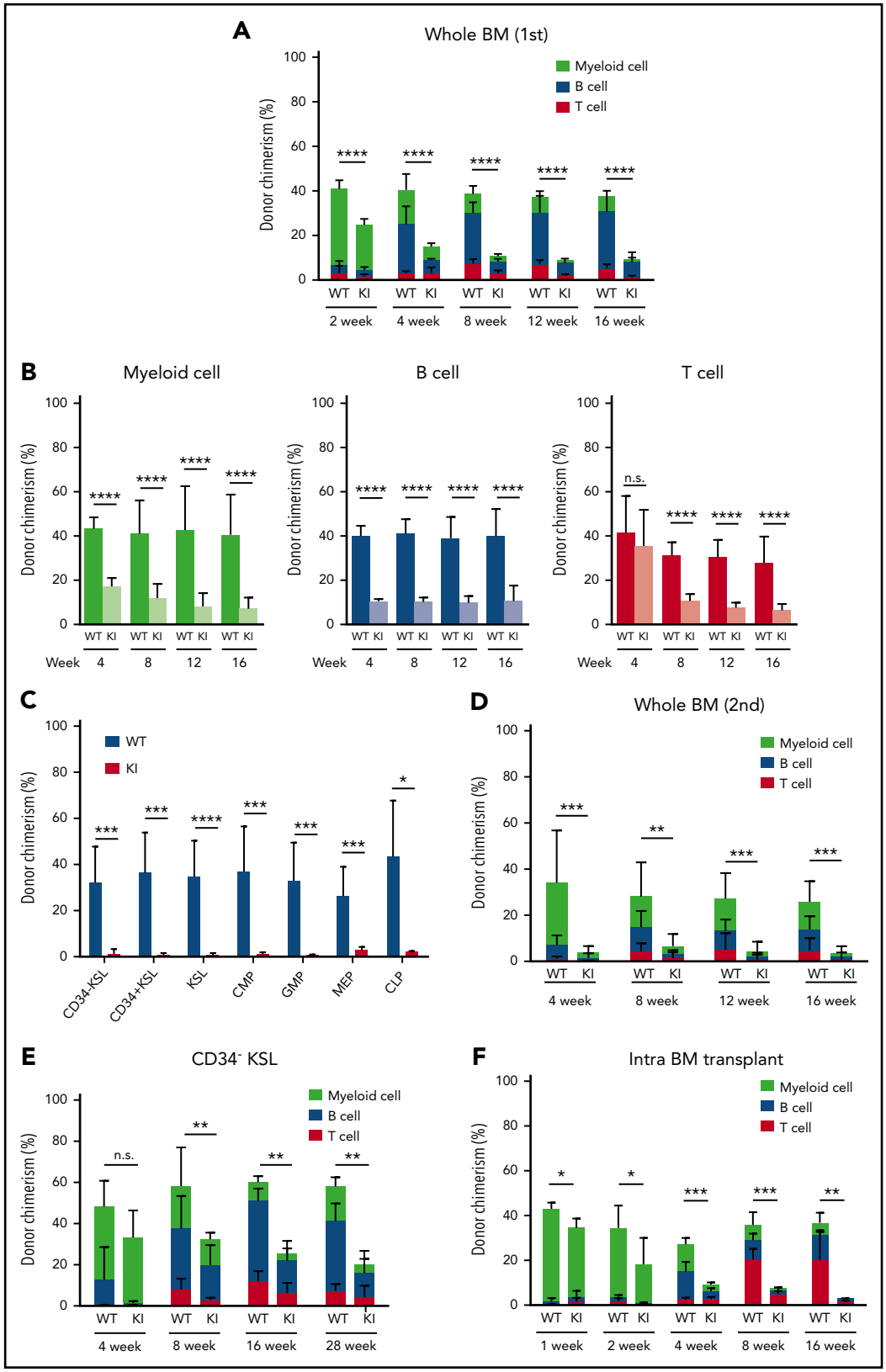

Figure 5. Compromised reconstitution capacity of *Srsf2*-mutated stem cells. (A) Percentage of CD45.2 donor cells in the PB of CD45.1 recipient mice after competitive transplantation using whole BM (mean ± SD, n = 10). (B) Chimerism of CD45.2 donor cells in myeloid (CD11b$^+$ and/or Gr-1$^+$), B-lymphoid (B220$^+$), and T-lymphoid (CD4$^+$ and/or CD8$^+$) cells in PB (mean ± SD, n = 10). (C) Donor chimerism of stem and progenitor cell fractions in BM 18 weeks after competitive BMT (mean ± SD, n = 7). (D) Percentage of CD45.2 donor cells in PB of CD45.1 recipients after secondary transplantation (mean ± SD, n = 10). (E) Percentage of CD45.2 donor cells in PB after competitive transplantation using enriched LT-HSCs (CD34$^-$KSL cells) (mean ± SD, n = 7). (F) Donor chimerism in PB after intra-BMT, indicated as mean ± SD (WT, n = 4; KI, n = 6). All of the transplantation experiments were performed in biological duplicate, and representative data are shown. *$P < .05$; **$P < .01$; ***$P < .001$; ****$P < .0001$. KI, *Srsf2* mutant transplanted mice; WT, wild-type transplanted mice.

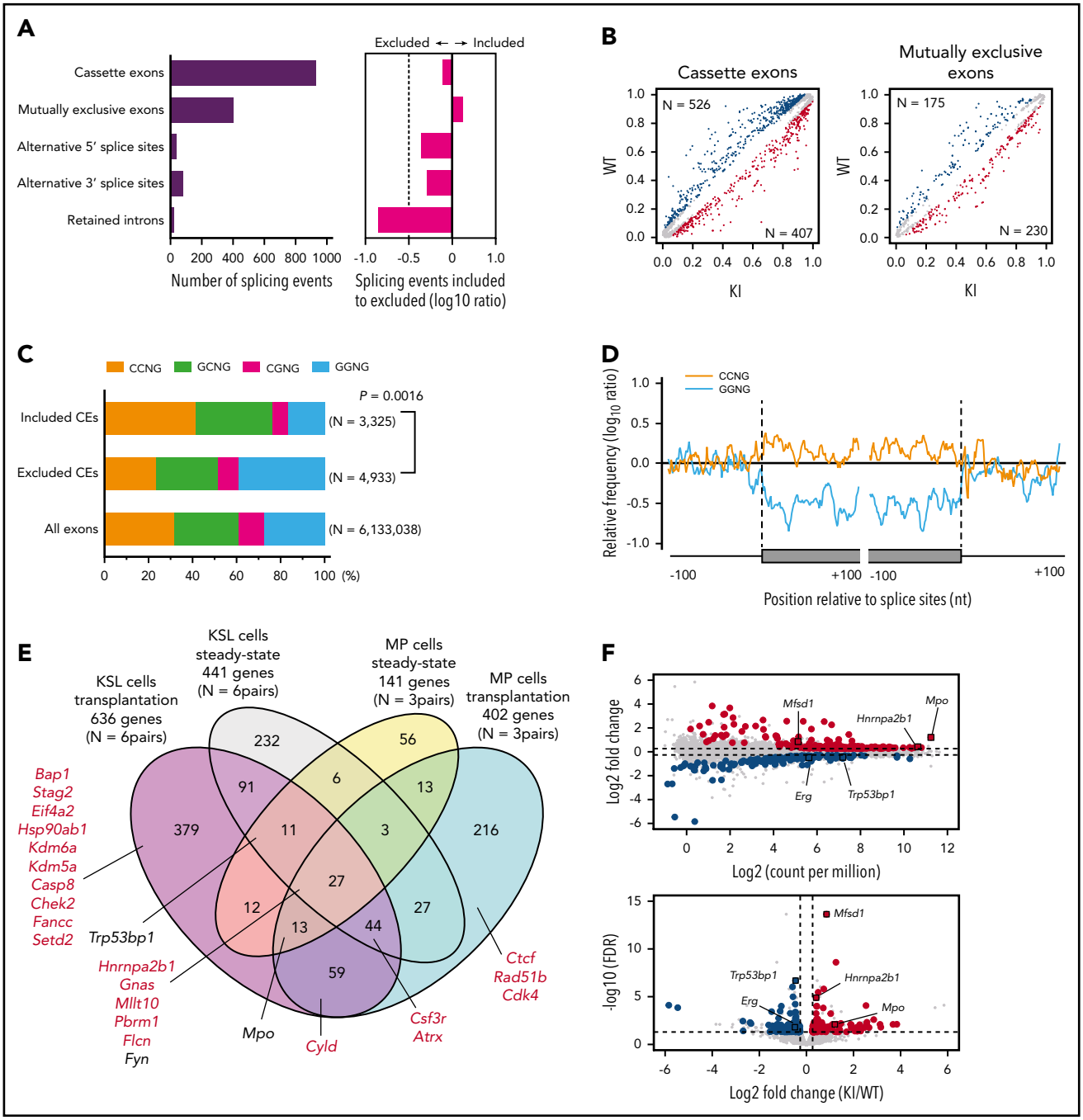

Figure 6. Effect of *Srsf2* P95H mutation on RNA splicing and expression in vivo. (A) Number of abnormal AS events identified in KSL cells of KI mice compared with that of WT mice in transplantation settings (n = 6 pairs). The $\log_{10}$ ratio of the number of abnormal AS events differentially included to those differentially excluded is also shown. (B) Inclusion levels of the CEs and mutually exclusive exons in KSL cells of KI mice compared with that of WT mice in transplantation settings are plotted. The colored dots represent significantly more included (red) and excluded (blue) events. The gray dots represent nonsignificant AS events with ≤5% inclusion level differences. (C) The composition of SSNG motifs in the more included or excluded CEs in the KSL cells of KI mice compared with that of WT mice in transplantation settings, and SSNG motif compositions in all of the exons from the mouse reference genome (mm10). (D) Relative frequency ($\log_{10}$ ratio) of the 7-base window-averaged number of CCNG and GGNG motifs in the CEs promoted vs repressed in KSL cells of KI mice, extending 100 nt into their upstream and downstream from the 5′ and 3′ splice sites. (E) Venn diagram comparing the differentially spliced genes between KI and WT cells from 4 different populations, ie, KSL and MP cells from the steady-state mice and those from the recipient mice in transplantation settings. Genes registered in the Cancer Gene Census are shown in red. (F) MA plot and volcano plot showing the transcriptional changes between KI and WT KSL cells in transplantation settings. Significantly upregulated and downregulated genes in KI cells compared with control cells are indicated by red and blue, respectively. (G) Venn diagram comparing the differentially upregulated (left) and downregulated (right) genes in Srsf2 mutant KSL and MP cells from the steady-state mice vs those from the recipient mice in transplantation settings. Genes registered in the Cancer Gene Census are shown in red. (H) Gene set enrichment analysis demonstrating a significant positive enrichment of gene sets upregulated in human MDS compared with healthy controls in *Srsf2* mutant KSL cells relative to wild-type KSL cells in transplantation settings (left panel), and negative enrichment of gene sets associated with the stemness (middle panel) and quiescence (right panel) in *Srsf2* mutant KSL cells relative to wild-type KSL cells under the steady-state conditions. Nominal *P* values, FDRs, and normalized enrichment scores (NSEs) are indicated. KI, Srsf2 mutant transplanted mice; WT, wild-type transplanted mice.

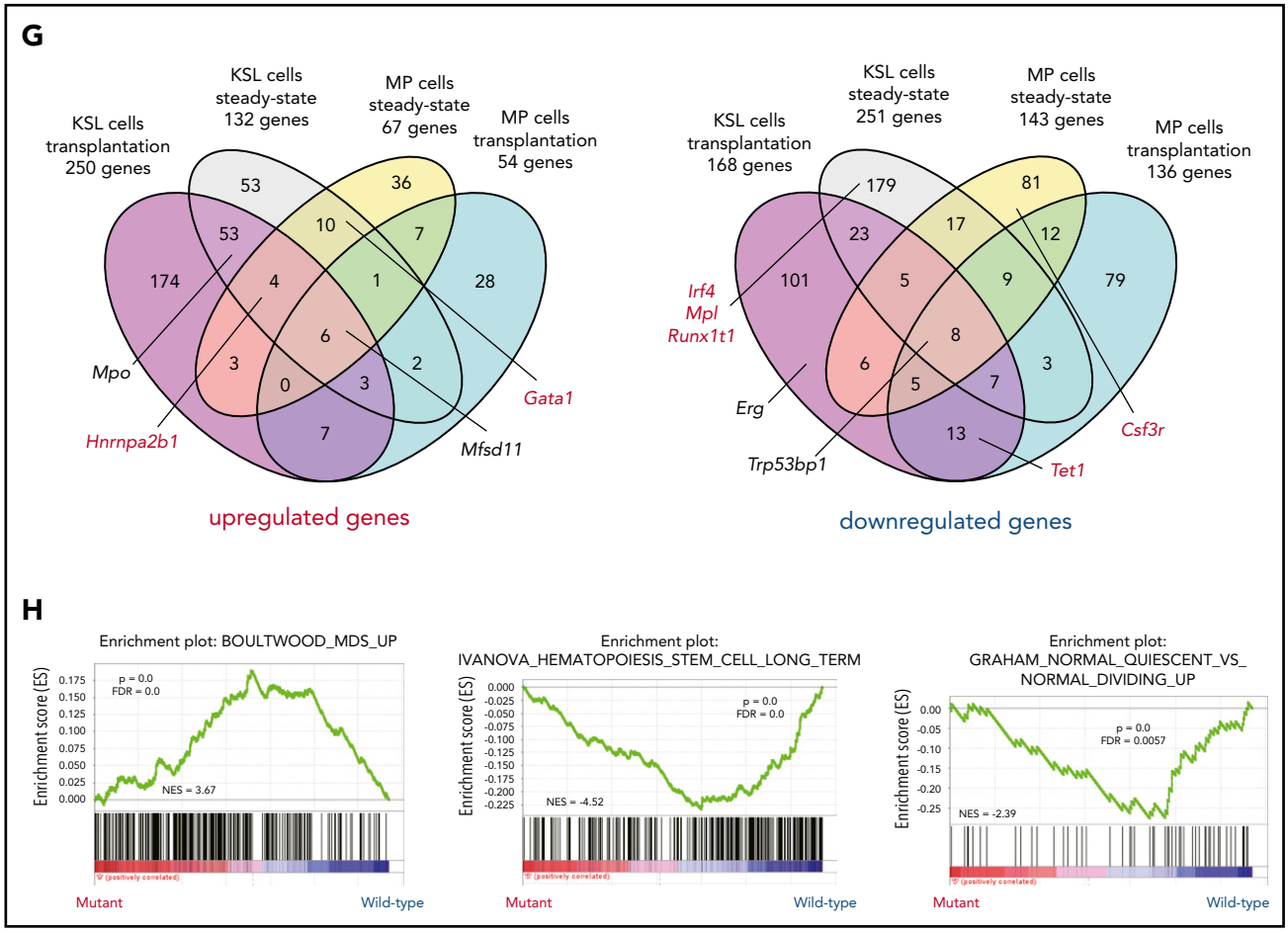

Figure 6. (Continued).

specifically favors SF-mutated HSCs may be among possible explanations.

In accordance with the previous study reported by Kim et al,[12] *Srsf2* mutant transplanted mice developed an MDS-like phenotype, showing leukopenia, anemia, and dysplastic morphologic features. A similar phenotype was also found in the steady-state condition, although the phenotype was much milder: No dysplastic phenotypes were observed, and only a mild decrease in hemoglobin was detected. Although the short life span of mouse models could limit the accumulation of genetic and/or epigenetic damages required for MDS development, it has been demonstrated that transplantation exposes cells to replicative stress by inducing rapid cycling of dormant HSCs, which leads to the accumulation of DNA damage in HSCs in a way that resembles age-associated effects.[35,36] Of interest is that higher numbers of abnormal AS events were observed in transplantation settings, where the targets of abnormal AS included those genes implicated in leukemogenesis, DNA damage response, and apoptosis. These findings suggest that mutant *Srsf2*-related abnormal AS is augmented by replicative stress, contributing to the enhanced MDS-like phenotype in *Srsf2* mutant mice in transplantation settings. This is also of interest in view of elderly onset of MDS and SF mutations associated with ARCH/CHIP.[50,51]

In sharp contrast to the previous study by Kim et al,[12] in which they reported increased numbers of HSPCs associated with mutant *Srsf2*, we found substantially reduced numbers of immature HSPCs both in the steady-state mouse BM and in the setting of transplantation. The reduced numbers of HSCs in our study, which were confirmed by limiting dilution experiments, seem to be in accordance with a reduced competitive repopulation capacity, increased cell cycling, and enhanced apoptosis, which might result in stem cell depletion. The precise reason for the differences between the present study and the study by Kim et al,[12] however, is still elusive. The effect of mutant *Srsf2* on the number of stem cells might be context dependent, in which the differences in the mutant construct (FLEx switch vs loxP-cDNA-STOP-loxP-mut cDNA), the Cre strain (*Vav1-Cre* vs *Mx1-Cre*) used for expression of the mutant allele, and/or the timing of mutant *Srsf2* expression in transplantation settings (before transplantation in our study; after transplantation in the study by Kim et al[12]) could be plausible explanations.

The functional targets of abnormal splicing responsible for the phenotype of *Srsf2*-mutated hematopoiesis are still elusive. Alternative CE usage should cause deletions or insertions of corresponding amino acids, likely resulting in loss of function of the protein in most cases, although the precise consequence is not necessarily easy to predict. As shown beforehand, the

Table 1. Differentially spliced genes in *Srsf2* mutant stem or progenitor cells for which mutations have been implicated in cancer

Gene	Splicing type	Reports from other authors			Tumor types
		Mouse model†	Human samples‡	Splicing type in human samples	
*Csf3r**	CE, MXE, A3SS	Yes	Yes	RI	CML, CNL, CMML, AML, MDS
*Gnas**	CE	Yes	Yes	CE	MDS, pituitary adenoma
Hnrnpa2b1	CE, MXE	Yes	Yes	CE	Prostate cancer
*Nsd1**	RI	Yes	Yes	RI	AML
Tpm3	CE	Yes	Yes	CE	Papillary thyroid cancer, lymphoma (ALCL), non–small cell lung cancer
Lmo2	MXE	Yes	Yes	CE	T-ALL
*Mllt10**	CE, MXE	Yes	No	—	Acute leukemia
*Atrx**	CE	No	No	—	MDS, pancreatic neuroendocrine tumors, pediatric glioblastoma
Tcf12	CE	No	No	—	Extraskeletal myxoid chondrosarcoma
Flcn	CE, A3SS	No	No	—	Renal carcinoma, fibrofolliculomas
Pbrm1	CE, MXE	No	No	—	Renal carcinoma, breast cancer
Ext2	CE, MXE	No	No	—	Exostoses, osteosarcoma
Tbl1xr1	CE, MXE	No	No	—	Lymphoma, gallbladder carcinoma

Among differentially spliced in more than 3 populations, 13 potential gene targets registered in the Cancer Gene Census (http://cancer.sanger.ac.uk/census) are listed.

A3SS, alternative 3′ splice sites; ALCL, anaplastic large-cell lymphoma; AML, acute myeloid leukemia; CML, chronic myeloid leukemia; CNL, chronic neutrophilic leukemia; MPN, myeloproliferative neoplasm; MXE, mutually exclusive exon; RI, retained intron; T-ALL, T-cell acute lymphoblastic leukemia.

*Genes implicated in the pathogenesis of myeloid malignancies.

†Reported in KSL or MP cell fractions from *Srsf2* P95H–mutated mice (Kim et al[12]).

‡Reported in human *SRSF2*-mutated AML or CMML samples (Kim et al[12]) and/or K562 cell lines harboring *SRSF2* P95H mutations (Zhang et al[13]).

consensus-binding motifs were substantially different between human and mouse, which might partly explain the different splicing patterns between the 2 species. Nevertheless, significant overlaps of the misspliced genes in *Srsf2*-mutated cells still existed between different mouse models and human cells, in which a number of genes implicated in human hematopoietic malignancies were affected; these included *Csf3r*, *Fyn*, *Gnas*, *Nsd1*, and *Hnrnpa2b1*. In addition, several genes underwent significant changes in both RNA splicing and expression between *Srsf2* mutant and wild-type cells, including *Hnrnpa2b1*, *Csf3r*, and *Trp53bp1*, which could be the candidates of functional targets of *Srsf2* mutation. Meanwhile, it is also unclear whether all of the hematological phenotypes associated with *Srsf2* mutants could be explained by abnormal splicing in a particular gene or set of genes. It might be also possible that a large number of abnormally spliced transcripts and consequent abnormal proteins, irrespective of the particular genes involved, cause compromised stem cell functions, contributing to MDS phenotypes. Further studies regarding these issues should be warranted.

In conclusion, the present study described the in vivo effects of the mutant *Srsf2* allele on the phenotypes of steady-state hematopoiesis, which were augmented in transplantation settings. *Srsf2* P95H mutation can cause abnormal RNA splicing typically of CEs and induce deregulation of HSCs, but it may not be sufficient to recapitulate a full picture of MDS at least in the steady-state condition. Our mouse model provides a valuable tool to understand the molecular pathogenesis of *Srsf2*-mutated myeloid neoplasms.

Figure 7. Comparisons of missplicedgenes in *Srsf2*-mutated cells between different mouse models and human cells. (A) Comparisons of missplicedgenes in KSL and MP cells from *Srsf2* mutant transplanted mice in the current study and those from *Mx1-Cre*–mediated *Srsf2* mutant mice (Kim et al[12]). Genes registered in the Cancer Gene Census are shown in red. Genes implicated in the pathogenesis of myeloid malignancies are marked with asterisks. (B) Comparisons of differentially spliced genes in KSL and MP cells from *Srsf2* mutant transplanted mice in the present study, *SRSF2*-mutated primary acute myeloid leukemia (AML) and CMML samples (Kim et al[12]), and K562 cell line transduced with mutant *SRSF2* (Zhang et al[13]). Genes registered in the Cancer Gene Census are shown in red. Genes implicated in the pathogenesis of myeloid malignancies are marked with asterisks. (C) Pie chart showing the number of promoted/repressed CEs in both KSL and MP cells from *Srsf2* mutant transplanted mice but not in *SRSF2* mutant human samples, with or without corresponding transcripts of the human orthologs. For those CEs who had human corresponding transcripts, the frequency of SSNG motifs (counts per kilobase) was compared between mice and humans.

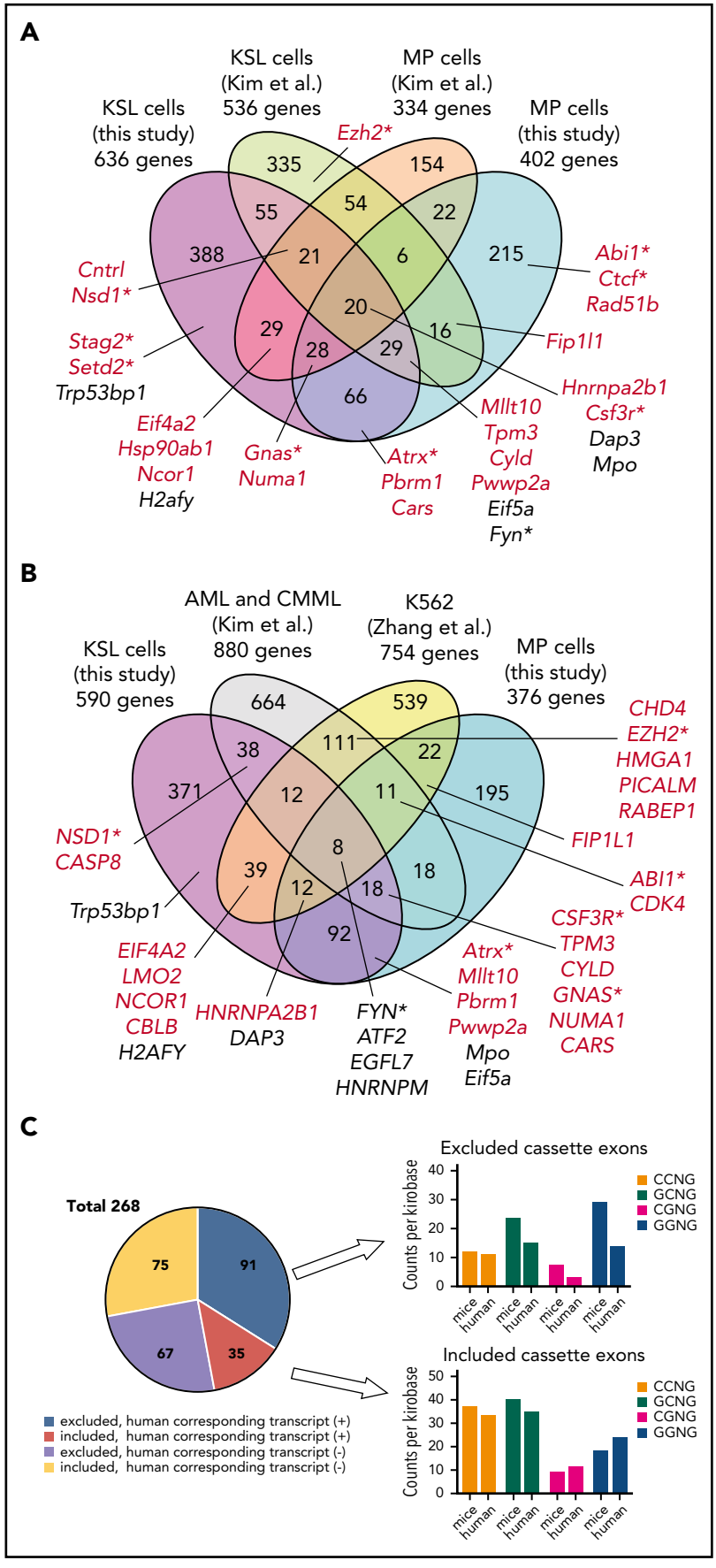

Acknowledgments

The authors thank Yuji Yamazaki for expert technical assistance in the fluorescence-activated cell-sorting operation; Hiroko Tsukui, Naomi Sato, Satoko Yabuta, Ai Takatsu, and Maki Nakamura for technical assistance; and Maiko Nakamura for precious secretarial assistance.

This work was supported by a Grant-in-Aid for Scientific Research (MEXT/JSPS KAKENHI JP26221308 and JP26253060 to S.O., JP16K19574 and JP14J03784 to A.K., and JP26115009 to M.S.); a Grant-in-Aid from the Japan Agency for Medical Research and Development (Project for Development of Innovative Research on Cancer Therapeutics [16cm0106501h0001 to S.O.], Practical Research for Innovative Cancer Control Project [15ck0106073h0002 and 16ck0106073h0003 to S.O.], and Strategic International Collaborative Research Program [16jm0210034h0104 to H.N.]); and grants from the Takeda Science Foundation (S.O.) and the Uehara Memorial Foundation (A.K.).

Authorship

Contribution: A.K. designed the study, analyzed the data, and wrote the manuscript; A.K. and S.Y. performed the animal experiments; A.K., M.S., and K.Y. performed the RNA-seq experiments; Y.N. and Y.S. performed bioinformatics analyses of the sequencing data; A.K. and Y.O. performed histopathological analyses; K.K. and M.M.N. provided the scientific discussion; M.M. and T.Y. assisted with the experiments; M.N. and H.K. generated *Srsf2* conditional knockin mice; H.N. and S.O. jointly supervised the project; and S.O. conceived and led the project, and wrote the manuscript.

Conflict-of-interest disclosure: The authors declare no competing financial interests.

ORCID profiles: A.K., 0000-0001-7237-0180; K.K., 0000-0002-8263-9902; M.M.N., 0000-0002-6420-2555; T.Y., 0000-0003-4283-2983; M.S., 0000-0003-0666-1996; H.K., 0000-0001-8424-5854; H.N., 0000-0002-8122-2566; S.O., 0000-0002-7778-5374.

Correspondence: Hiromitsu Nakauchi, Institute for Stem Cell Biology and Regenerative Medicine, Stanford University School of Medicine, 265 Campus Dr, Stanford, CA 94305; e-mail: nakauchi@stanford.edu; and Seishi Ogawa, Department of Pathology and Tumor Biology, Graduate School of Medicine, Kyoto University, Yoshida-Konoe-cho, Sakyo-ku, Kyoto-shi, Kyoto 606-8501, Japan; e-mail: sogawa-tky@umin.ac.jp.

Footnotes

Submitted 13 January 2017; accepted 9 November 2017. Prepublished online as *Blood* First Edition paper, 16 November 2017; DOI 10.1182/blood-2017-01-762393.

*H.N. and S.O. contributed equally to this study.

The sequencing data reported in this article have been deposited in the DNA Data Bank of Japan Sequence Read Archive (accession number DRA006224).

The online version of this article contains a data supplement.

The publication costs of this article were defrayed in part by page charge payment. Therefore, and solely to indicate this fact, this article is hereby marked "advertisement" in accordance with 18 USC section 1734.

REFERENCES

1. Adès L, Itzykson R, Fenaux P. Myelodysplastic syndromes. *Lancet*. 2014;383(9936):2239-2252.
2. Tefferi A, Vardiman JW. Myelodysplastic syndromes. *N Engl J Med*. 2009;361(19):1872-1885.
3. Papaemmanuil E, Gerstung M, Malcovati L, et al Chronic Myeloid Disorders Working Group of the International Cancer Genome Consortium. Clinical and biological implications of driver mutations in myelodysplastic syndromes. *Blood*. 2013;122(22):3616-3627, quiz 3699.
4. Haferlach T, Nagata Y, Grossmann V, et al. Landscape of genetic lesions in 944 patients with myelodysplastic syndromes. *Leukemia*. 2014;28(2):241-247.
5. Yoshida K, Sanada M, Shiraishi Y, et al. Frequent pathway mutations of splicing machinery in myelodysplasia. *Nature*. 2011;478(7367):64-69.
6. Graveley BR, Maniatis T. Arginine/serine-rich domains of SR proteins can function as activators of pre-mRNA splicing. *Mol Cell*. 1998;1(5):765-771.
7. Bradley T, Cook ME, Blanchette M. SR proteins control a complex network of RNA-processing events. *RNA*. 2015;21(1):75-92.
8. Daubner GM, Cléry A, Jayne S, Stevenin J, Allain FH. A syn-anti conformational difference allows SRSF2 to recognize guanines and cytosines equally well. *EMBO J*. 2012;31(1):162-174.
9. Meggendorfer M, Roller A, Haferlach T, et al. SRSF2 mutations in 275 cases with chronic myelomonocytic leukemia (CMML). *Blood*. 2012;120(15):3080-3088.
10. Patnaik MM, Lasho TL, Finke CM, et al. Spliceosome mutations involving SRSF2, SF3B1, and U2AF35 in chronic myelomonocytic leukemia: prevalence, clinical correlates, and prognostic relevance. *Am J Hematol*. 2013;88(3):201-206.
11. Itzykson R, Kosmider O, Renneville A, et al. Clonal architecture of chronic myelomonocytic leukemias. *Blood*. 2013;121(12):2186-2198.
12. Kim E, Ilagan JO, Liang Y, et al. SRSF2 mutations contribute to myelodysplasia by mutant-specific effects on exon recognition. *Cancer Cell*. 2015;27(5):617-630.
13. Zhang J, Lieu YK, Ali AM, et al. Disease-associated mutation in SRSF2 misregulates splicing by altering RNA-binding affinities. *Proc Natl Acad Sci USA*. 2015;112(34):E4726-E4734.
14. Shirai CL, Ley JN, White BS, et al. Mutant U2AF1 expression alters hematopoiesis and Pre-mRNA splicing in vivo. *Cancer Cell*. 2015;27(5):631-643.
15. Obeng EA, Chappell RJ, Seiler M, et al. Physiologic expression of Sf3b1(K700E) causes impaired erythropoiesis, aberrant splicing, and sensitivity to therapeutic spliceosome modulation. *Cancer Cell*. 2016;30(3):404-417.
16. Mupo A, Seiler M, Sathiaseelan V, et al. Hemopoietic-specific Sf3b1-K700E knock-in mice display the splicing defect seen in human MDS but develop anemia without ring sideroblasts. *Leukemia*. 2017;31(3):720-727.
17. Suzuki E, Nakayama M. VCre/VloxP and SCre/SloxP: new site-specific recombination systems for genome engineering. *Nucleic Acids Res*. 2011;39(8):e49.
18. Schnütgen F, Doerflinger N, Calléja C, Wendling O, Chambon P, Ghyselinck NB. A directional strategy for monitoring Cre-mediated recombination at the cellular level in the mouse. *Nat Biotechnol*. 2003;21(5):562-565.
19. Ema H, Morita Y, Yamazaki S, et al. Adult mouse hematopoietic stem cells: purification and single-cell assays. *Nat Protoc*. 2006;1(6):2979-2987.
20. Kim D, Langmead B, Salzberg SL. HISAT: a fast spliced aligner with low memory requirements. *Nat Methods*. 2015;12(4):357-360.
21. Shen S, Park JW, Lu ZX, et al. rMATS: robust and flexible detection of differential alternative splicing from replicate RNA-Seq data. *Proc Natl Acad Sci USA*. 2014;111(51):E5593-E5601.
22. Liao Y, Smyth GK, Shi W. The Subread aligner: fast, accurate and scalable read mapping by seed-and-vote. *Nucleic Acids Res*. 2013;41(10):e108.
23. Robinson MD, McCarthy DJ, Smyth GK. edgeR: a Bioconductor package for differential expression analysis of digital gene expression data. *Bioinformatics*. 2010;26(1):139-140.
24. McCarthy DJ, Chen Y, Smyth GK. Differential expression analysis of multifactor RNA-Seq experiments with respect to biological variation. *Nucleic Acids Res*. 2012;40(10):4288-4297.
25. de Boer J, Williams A, Skavdis G, et al. Transgenic mice with hematopoietic and lymphoid specific expression of Cre. *Eur J Immunol*. 2003;33(2):314-325.
26. Essers MA, Offner S, Blanco-Bose WE, et al. IFNalpha activates dormant haematopoietic

stem cells in vivo. *Nature*. 2009;458(7240):904-908.

27. Baldridge MT, King KY, Boles NC, Weksberg DC, Goodell MA. Quiescent haematopoietic stem cells are activated by IFN-gamma in response to chronic infection. *Nature*. 2010;465(7299):793-797.

28. Osawa M, Hanada K, Hamada H, Nakauchi H. Long-term lymphohematopoietic reconstitution by a single CD34-low/negative hematopoietic stem cell. *Science*. 1996;273(5272):242-245.

29. Kiel MJ, Yilmaz OH, Iwashita T, Yilmaz OH, Terhorst C, Morrison SJ. SLAM family receptors distinguish hematopoietic stem and progenitor cells and reveal endothelial niches for stem cells. *Cell*. 2005;121(7):1109-1121.

30. Oguro H, Ding L, Morrison SJ. SLAM family markers resolve functionally distinct subpopulations of hematopoietic stem cells and multipotent progenitors. *Cell Stem Cell*. 2013;13(1):102-116.

31. Akashi K, Traver D, Miyamoto T, Weissman IL. A clonogenic common myeloid progenitor that gives rise to all myeloid lineages. *Nature*. 2000;404(6774):193-197.

32. Kondo M, Weissman IL, Akashi K. Identification of clonogenic common lymphoid progenitors in mouse bone marrow. *Cell*. 1997;91(5):661-672.

33. Sitnicka E, Buza-Vidas N, Ahlenius H, et al. Critical role of FLT3 ligand in IL-7 receptor independent T lymphopoiesis and regulation of lymphoid-primed multipotent progenitors. *Blood*. 2007;110(8):2955-2964.

34. Challen GA, Sun D, Jeong M, et al. Dnmt3a is essential for hematopoietic stem cell differentiation. *Nat Genet*. 2011;44(1):23-31.

35. Flach J, Bakker ST, Mohrin M, et al. Replication stress is a potent driver of functional decline in ageing haematopoietic stem cells. *Nature*. 2014;512(7513):198-202.

36. Walter D, Lier A, Geiselhart A, et al. Exit from dormancy provokes DNA-damage-induced attrition in haematopoietic stem cells. *Nature*. 2015;520(7548):549-552.

37. Sternberg A, Killick S, Littlewood T, et al. Evidence for reduced B-cell progenitors in early (low-risk) myelodysplastic syndrome. *Blood*. 2005;106(9):2982-2991.

38. Socolovsky M, Nam H, Fleming MD, Haase VH, Brugnara C, Lodish HF. Ineffective erythropoiesis in Stat5a(-/-)5b(-/-) mice due to decreased survival of early erythroblasts. *Blood*. 2001;98(12):3261-3273.

39. Fox SB, Lorenzen J, Heryet A, Jones M, Gatter KC, Mason DY. Megakaryocytes in myelodysplasia: an immunohistochemical study on bone marrow trephines. *Histopathology*. 1990;17(1):69-74.

40. Shen H, Green MR. RS domains contact splicing signals and promote splicing by a common mechanism in yeast through humans. *Genes Dev*. 2006;20(13):1755-1765.

41. Pandit S, Zhou Y, Shiue L, et al. Genome-wide analysis reveals SR protein cooperation and competition in regulated splicing. *Mol Cell*. 2013;50(2):223-235.

42. Subramanian A, Tamayo P, Mootha VK, et al. Gene set enrichment analysis: a knowledge-based approach for interpreting genome-wide expression profiles. *Proc Natl Acad Sci USA*. 2005;102(43):15545-15550.

43. Mootha VK, Lindgren CM, Eriksson KF, et al. PGC-1alpha-responsive genes involved in oxidative phosphorylation are coordinately downregulated in human diabetes. *Nat Genet*. 2003;34(3):267-273.

44. Pellagatti A, Cazzola M, Giagounidis A, et al. Deregulated gene expression pathways in myelodysplastic syndrome hematopoietic stem cells. *Leukemia*. 2010;24(4):756-764.

45. Lavallée VP, Krosl J, Lemieux S, et al. Chemogenomic interrogation of CEBPA mutated AML reveals recurrent CSF3R mutations and subgroup sensitivity to JAK inhibitors. *Blood*. 2016;127(24):3054-3061.

46. Maxson JE, Gotlib J, Pollyea DA, et al. Oncogenic CSF3R mutations in chronic neutrophilic leukemia and atypical CML. *N Engl J Med*. 2013;368(19):1781-1790.

47. Chougule RA, Kazi JU, Rönnstrand L. FYN expression potentiates FLT3-ITD induced STAT5 signaling in acute myeloid leukemia. *Oncotarget*. 2016;7(9):9964-9974.

48. Bejar R, Stevenson K, Abdel-Wahab O, et al. Clinical effect of point mutations in myelodysplastic syndromes. *N Engl J Med*. 2011;364(26):2496-2506.

49. Wang GG, Cai L, Pasillas MP, Kamps MP. NUP98-NSD1 links H3K36 methylation to Hox-A gene activation and leukaemogenesis. *Nat Cell Biol*. 2007;9(7):804-812.

50. Xie M, Lu C, Wang J, et al. Age-related mutations associated with clonal hematopoietic expansion and malignancies. *Nat Med*. 2014;20(12):1472-1478.

51. McKerrell T, Park N, Moreno T, et al; Understanding Society Scientific Group. Leukemia-associated somatic mutations drive distinct patterns of age-related clonal hemopoiesis. *Cell Reports*. 2015;10(8):1239-1245.

52. Jaiswal S, Fontanillas P, Flannick J, et al. Age-related clonal hematopoiesis associated with adverse outcomes. *N Engl J Med*. 2014;371(26):2488-2498.

53. Genovese G, Kähler AK, Handsaker RE, et al. Clonal hematopoiesis and blood-cancer risk inferred from blood DNA sequence. *N Engl J Med*. 2014;371(26):2477-2487.

54. Steensma DP, Bejar R, Jaiswal S, et al. Clonal hematopoiesis of indeterminate potential and its distinction from myelodysplastic syndromes. *Blood*. 2015;126(1):9-16.